THE STRUCTURE OF INHIBITED COUNTERFLOWING NONPREMIXED FLAMES

Anthony Hamins[1], Ming Hua Yang[2], and Ishwar K. Puri[2]
[1]Building and Fire Research Laboratory
National Institute of Standards and Technology
Gaithersburg, Maryland 20899
and
[2]Department of Mechanical Engineering (M/C 251)
University of Illinois at Chicago
Chicago, Illinois 60607-7022

INTRODUCTION

Recent international agreements call for a halt to the manufacture of CF_3Br (Halon 1301), a commonly used halon fire suppressant, due to its high ozone-depletion potential. Ideally, the search for replacement compounds should be guided by fundamental studies of the detailed inhibition mechanisms of halogenated agents in flames. A large number of experimental and modeling studies have investigated the impact of halogenated inhibitors in premixed systems. Few studies, however, have investigated the detailed structure of nonpremixed flames with chemical inhibitors added to the oxidizer stream, a configuration that more closely corresponds to realistic fire situations. In an effort to construct a paradigm of flame inhibition by halogenated compounds, an experimental and numerical investigation of the effect of chloromethane addition to the oxidizer stream of counterflowing nonpremixed flames was conducted.

Flame Suppression

Because premixed and nonpremixed flame structures are different, it is not clear that the kinetic channels that lead to flame extinction in these two configurations are identical. The temperature and concentration gradients are relatively gradual in premixed flames, whereas in nonpremixed flames, these gradients are steep and transport processes may play a limiting role in the extinction process. Typical fire situations correspond to nonpremixed combustion with fire suppressants added to the oxidizer stream of a nonpremixed flame.

A number of experimental and modeling studies have focused on the impact of halogenated inhibitors on hydrocarbon combustion in flow reactors, flow tubes, premixed flames, shock tubes, and fluidized beds. In general, it is thought that halogenated compounds scavenge radical species, deplete the radical pool, and inhibit key chemical reactions. The details of the inhibition mechanism depend on a number of parameters which represent local flame conditions such as the temperature, equivalence ratio, and pressure.

In nonpremixed flames, previous investigations have been almost exclusively experimental. The suppression effectiveness of halogenated chemicals has been studied phenomenologically, in counterflow flames (Seshadri, 1976) and in co-flow flames (Creitz, 1961; Tucker et al., 1981;). A global measure of the chemical effectiveness of an agent has been quantified through heat capacity considerations (Tucker et al., 1981; Sheinson et al., 1989). A limited number of flame structure measurements have been conducted in inhibited nonpremixed flames, including measurements of both stable and some radical chemical species. Yet, there have been no quantitative studies investigating the chemical routes associated with chemical inhibition in nonpremixed flames.

Objectives

The objective of the current study is to investigate the changes

that occur in flame structure upon addition of a halogenated compound into the oxidizer stream of a nonpremixed flame, and to relate these changes to the inhibition mechanism. Chemical inhibition is contrasted to physical suppression and to a flame with enhanced stability by investigating the flame structures with an inert or a fuel, respectively, added to the oxidizer stream of the nonpremixed flame.

METHODOLOGY

The chemical species, nitrogen (N_2), chloromethane (CH_3Cl), and methane (CH_4) were chosen as "agents" and were introduced into the oxidizer stream of a CH_4-air nonpremixed flame that is referred to as the "base" flame. Chloromethane was chosen because an adequate amount of thermophysical and kinetic data are available. Methane was studied because its molecular structure is highly similar to chloromethane and because its addition to the flame (as with chloromethane) increases the enthalpy of the system. Whereas methane addition causes a nonpremixed flame to become more stable, chloromethane addition inhibits the flame.

Numerical simulations of flame structure for the cases of 5% N_2, 10% N_2, and 5% CH_3Cl added to the oxidizer stream were compared to experimental measurements of the velocity and temperature fields. In addition, the critical concentrations of N_2 and CH_3Cl in the oxidizer stream needed to extinguish the methane-air flame were measured. For all flames, the strain rate, determined from the axial velocity gradient on the oxidizer side of the high temperature reaction zone, was maintained at $\approx 98\ s^{-1}$.

Numerical Method

Numerical simulations of laminar counterflow flames were performed using a previously developed computer code [Rogg, 1991]. The code allows for the calculation of the structure of laminar flames using detailed models of molecular transport and chemical kinetics. The kinetic mechanism used is from Miller and Bowman [1989] for methane oxidation and from Barat et al. [1990] for chloromethane combustion. The mechanism includes 179 elementary forward reactions involving 38 gas-phase species including C_2 species. The backward rates are calculated from thermodynamic equilibrium [Rogg, 1991]. Radiative losses are not included, but are expected to be inconsequential for these thin nonsooting flames [Sohrab et al., 1982]. A complete description of the computation is described elsewhere [Lee et al., 1993; Lee and Puri, 1993]. For convenience, the numbering system in those studies is maintained here. The kinetic scheme has been employed to predict successfully the flame speed of unstretched premixed flames burning chloromethane-air mixtures and the extinction of counterflowing nonpremixed flames burning mixtures of methane and chloromethane [Huh and Puri, 1993; Lee et al., 1993; Yang and Puri, 1993].

EXPERIMENTAL METHOD

Figure 1 is a schematic drawing of the counterflow burner. The inner diameter of the opposed jets was 25.4 mm and the duct separation distance was 15 mm. Gas flow rates were controlled by calibrated rotameters. The experimental arrangement has been previously described [Lee et al., 1993; Huh et al., 1993; Yang and Puri, 1993]. Velocity measurements were made with a laser doppler velocimeter/particle analyzer using the method described previously (Lee et al., 1993; Yang and Puri, 1993). The flow was seeded with magnesium oxide particles (≈1-

5μ diameter). A 500 mW argon-ion laser was used to illuminate the measurement volume and the signal was monitored in back scatter mode. A Bragg Cell was employed to measure velocities throughout the flow field including locations near the stagnation point. Temperature measurements were made using Pt/Pt-10% Rh thermocouples (0.076 mm diameter) coated with Yttrium Oxide to reduce catalytic effects. Radiation corrections to the temperature data were applied following the method outlined by Fristrom and Westenberg [1965]. A more detailed discussion of the radiation correction can be found in Huh et al. [1993].

RESULTS AND DISCUSSION

Comparison of Measurements with the Structure of Simulated Flames

Figure 2 compares the measured and calculated axial velocity profiles as a function of distance from the oxidizer duct for the flame with 5% CH_3Cl added to the oxidizer stream. The stagnation plane is located approximately 9 mm from the oxidizer duct. Velocity measurements on the base flame, and the flames with 5% and 10% N_2 added to the oxidizer stream show good agreement with the calculated velocity profiles.

Figure 3 shows the measured axial temperature as a function of distance from the oxidizer duct for the flame with 5% CH_3Cl added to the oxidizer stream. Also shown are the measurements corrected for radiative heat losses and the calculated temperature profiles. Good agreement between the calculated and radiation corrected temperature profiles is also found for the base flame and the flames with 5% N_2, and 10% N_2 added to the oxidizer stream.

Comparison of the Detailed Structure of Simulated Flames

Figure 4 compares the computed temperature profiles for the base flame and for the flames with 5% N_2, 10% N_2, 5% CH_3Cl, and 5% CH_4 added to the oxidizer stream. The peak flame temperature decreased with N_2 addition, whereas the spatial location of the maximum was unaltered. In contrast, the addition of CH_4 and CH_3Cl broadened the temperature profile, increased the maximum temperature, and shifted the peak towards the oxidizer side of the flame. The increased flame temperature is attributed to the increased enthalpy associated with CH_3Cl and CH_4 addition. The broadened peak for the CH_3Cl addition flame (as compared to the base flame) was also observed experimentally.

Figure 5 shows the concentration of major chlorinated species as a function of location in the flame when 5% CH_3Cl was added to the oxidizer stream. As CH_3Cl pyrolyzes, a series of reactions lead to the formation of HCl and Cl. Figure 5 also displays the complete local equilibrium for HCl (based on local temperature and composition) which shows that HCl is nearly in equilibrium at all locations near the high temperature reaction zone [Gordon and McBride, 1976]. A dip in the HCl concentration occurs approximately 6 mm from the oxidizer duct and is related to fast bimolecular processes involving OH·, H atom, and O atom which destroy HCl. The Cl atom concentration in Fig. 5 is larger than the OH·, H atom or O atom concentrations and is in super-equilibrium, not unlike other flame radicals.

Figure 6 compares the calculated OH· concentrations, for the flames with 5% N_2, 10% N_2, 5% CH_3Cl, and 5% CH_4 added to the oxidizer stream. In the flames with N_2 addition, the radical concentration decreased, whereas the location of the peak remained unchanged. This was linked to the decreased temperatures in these flames. Methane addition had a very

different effect, yielding increased radical concentrations consistent with increased flame temperatures. In contrast, the OH· concentration decreased with CH_3Cl addition, despite increased flame temperatures. Similar results were found for H and O atoms. The mechanism associated with the depletion of the radical pool by a halogenated compound is discussed below.

Reaction Path Analysis of the Simulated Flames

Figure 7 shows the net OH· formation rates as a function of location for the fastest reactions in the flame with 5% CH_3Cl added to the oxidizer stream. The net rate is defined as the forward rate minus the backward rate for the same reaction. Table 1 lists reactions pertinent to Fig. 7 and the following discussion. Consideration of the net rates, allows evaluation of the relative importance of key reactions in the production (or destruction) of a particular species. Figure 7 indicates which reactions are responsible for decreases in the OH· concentration. The negative net rates for reactions (R305-R306) and (R279-R280) exemplify the role of chlorinated compounds in reactions which lead to decreases in OH· concentration. The magnitude of the net rate (R279-R280) is of the same order as the net rate (R305-R306). These OH· destruction processes are even faster than (R211-R212), which is the fastest reaction pair involving a nonchlorinated species.

The OH· reaction with HCl (R305) is fast on the oxidizer side of the high temperature reaction zone, leading to the production of Cl atoms. Reaction R299 is also prominent in the high temperature reaction zone, consuming H and Cl atoms and producing HCl. A sum of the reactions (R299 plus R305) yields the effective chain termination reaction:

R305	$HCl + OH\cdot \rightarrow Cl + H_2O$
+ R299	$H + Cl + M \rightarrow HCl + M$
sum	$H + OH\cdot \rightarrow H_2O$

where two reactive species combine into a relatively unreactive compound.

An analysis of the key H atom formation rates suggests that decreases in the H atom concentration is due to chlorinated species reacting through (R301-R302) and the three-body termination reaction (R299-R300). These same processes (R301, R305, and R299) are also important in the inhibition of methane-air premixed flames with chloromethane addition (Lee and Puri, 1993).

Chlorine Pathways in the Simulated Flame

Figure 8 is a schematic representation of the dominant chemical pathways involved in chloromethane pyrolysis, determined from a reaction path analysis. CH_3Cl destruction is dominated by R257 (see the Table) where CH_3Cl reacts with Cl atoms leading to the formation of HCl and CH_2Cl. CH_2Cl destruction occurs principally through reaction with OH· (via R279) which leads to the formation of HCl and CH_2O. CH_2O can react with Cl via R281 to form HCl. Thus, CH_3Cl pyrolysis leads to the formation of HCl either directly (R257) or through CH_2Cl (via R279) or CH_2O (via R281). HCl is also produced by R299, the three body chain termination reaction where H atom, Cl atom, and a third body combine. Once HCl is formed, fast bimolecular reactions (R302, R303, and R305) involving OH·, H atom, and O atom lead to HCl destruction and Cl atom formation.

CONCLUSIONS

In an effort to construct a paradigm for flame inhibition by halogenated compounds, an experimental and numerical investigation of the effect of chloromethane addition to the oxidizer stream of counterflowing nonpremixed flames was conducted. Measured temperature and velocity profiles compared favorably to the calculated flame structures. The calculated flame structures were then used to perform a reaction path analysis of the inhibition mechanisms associated with chloromethane. These results were compared to the effects of inert nitrogen. Analysis of the calculated flame structures suggest:

1. Chloromethane addition to the oxidizer stream dramatically alters the flame structure, causing decreased concentrations of key flame radicals (H atom, O atom, and OH·) and increased flame temperatures. Decreased radical concentrations are due principally to the reaction of radicals with HCl throughout the high temperature reaction zone.
2. Nitrogen addition to the oxidizer stream lowers the flame temperature and thereby perturbs the rate of important bimolecular reactions, leading to decreased OH·, O atom, and H atom concentrations.
3. Many of the same inhibition processes that occur in premixed flames are also important in the moderately strained nonpremixed flames studied here.

ACKNOWLEDGEMENTS

A. Hamins is supported by the U.S. Air Force, Wright Patterson AFB under the direction of M. Bennett. M.H. Yang and I.K. Puri are supported by U.S. EPA through Grant No. R-816856-01-0. The authors are very grateful to Professor J.W. Bozelli of the New Jersey Institute of Technology for extremely helpful discussions and to Professor S. Senkan of the University of California at Los Angeles for providing a portion of the thermodynamic and molecular database used in these calculations.

REFERENCES

Barat, R.B. Sarofim, A.F., Longwell, J.P. and Bozelli, J.W., Combust. Sci. Tech., **74**:361 (1990).

Creitz, E.C., J. Research National Bureau Stand., **65A**:389 (1961).

Fristrom, R.M., and Westenberg, A.A., Flame Structure, McGraw Hill, New York, 1965, pp.145-176.

Gordon, S. and McBride, B.J., *Computer program for calculation of complex chemical equilibrium compositions, rocket performance, incident and reflected shocks, and Chapman-Jouget detonations.* NASA, March 1976. NASA SP-273 (1976).

Huh, J.Y., and Puri, I.K. (1993). *Radiation corrections applied to thermocouple measurements in nonpremixed flames,* Combust. Flame (submitted).

Huh, J.Y., Lee, K.Y. and Puri, I.K. (1993). *The structure and extinction of nonpremixed methyl chloride/methane air flames,* Combust. Flame (submitted).

Lee, K.Y., Yang, M.H. and Puri, I.K., Combust. Flame, **92**:419 (1993).

Lee, K.Y. and Puri, I.K., Combust. Flame, **92**:440 (1993).

Miller, J.A. and Bowman, C.T., Prog. Energy Combust. Sci., **15**:287 (1989).

Rogg, B. (1991). RUN-1DS: A computer program for the simulation of one-dimensional chemically reacting flows. Technical Report CUED/A-THERMO/TR39, University of Cambridge, Department of Engineering.

Seshadri, K., and Williams, F.A., in Halogenated Fire Suppressants, R.G. Gann (Ed.), ACS Symposium 16, Am. Chem. Soc., pp. 149-182, Washington, D.C., 1975.

Sohrab, S.H., Linan, A., and Williams, F.A., Combust. Sci. Tech. 27:143 (1982).

Sheinson, R.S., Penner-Hahn, J., and D. Indritz, Fire Safety J. 15:437 (1989).

Tucker, D.M., Drysdale, D.D. and Rasbash, D.J., Combust. Flame, 41:293 (1981).

Yang, M.H. and Puri, I.K. (1993). *Experimental Investigation of stretched premixed flames burning methyl chloride and methane in air and comparison with numerical simulations*, Combust. Flame (accepted for publication).

Yang, M.H., Puri, I.K. and Hamins, A. (1993). *The structure of inhibited, diluted, and stretched Flames*, Paper #4, Eastern and Central States Sections Meeting of the Combustion Institute. New Orleans, LA.

Table 1. Pertinent reactions.

Number	Reaction
R211	$OH\cdot + H_2 \rightarrow H_2O + H$
R212	$H_2O + H \rightarrow H_2 + OH\cdot$
R213	$O + OH\cdot \rightarrow O_2 + H$
R214	$O_2 + H \rightarrow O + OH\cdot$
R215	$O + H_2 \rightarrow OH\cdot + H$
R257	$CH_3Cl + Cl \rightarrow CH_2Cl + HCl$
R279	$CH_2Cl + OH\cdot \rightarrow HCl + CH_2O$
R280	$HCl + CH_2O \rightarrow CH_2Cl + OH\cdot$
R281	$CH_2O + Cl \rightarrow HCl + HCO$
R299	$Cl + H + M \rightarrow HCl + M$
R300	$HCl + M \rightarrow H + Cl + M$
R301	$Cl + H_2 \rightarrow HCl + H$
R302	$HCl + H \rightarrow Cl + H_2$
R303	$HCl + O \rightarrow Cl + OH\cdot$
R304	$Cl + OH\cdot \rightarrow HCl + O$
R305	$HCl + OH\cdot \rightarrow Cl + H_2O$
R306	$Cl + H_2O \rightarrow HCl + OH\cdot$

University of New Mexico; New Mexico Engineering Research Institute; Center for Global Environmental Technologies; National Association of Fire Equipment Distributors, Inc.; Halon Alternative Research Corp.; Fire Suppression Systems Assoc.; and Hughes Associates, Inc. Halon Alternatives Technical Working Conference 1993. Proceedings. May 11-13, 1993, Albuquerque, NM, 503-510 pp, 1993.

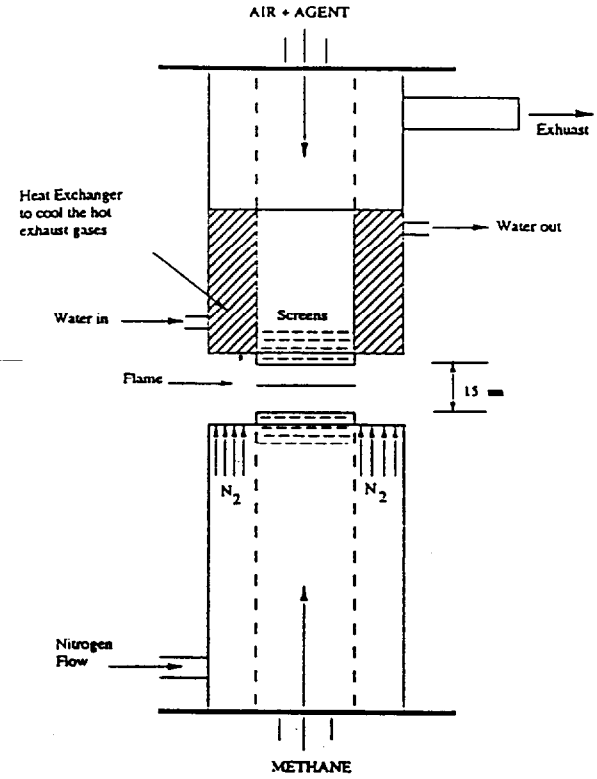

1. *Schematic diagram of the counterflow burner.*

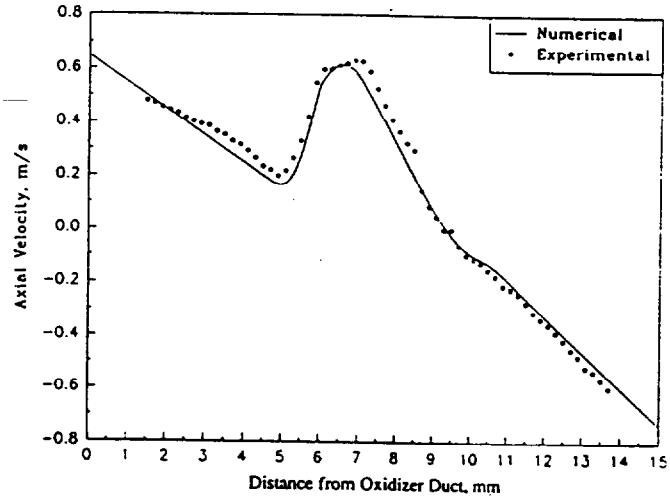

2. *The measured (points) and calculated (line) velocities as a function of location in the flame with 5% CH_3Cl added to the oxidizer stream.*

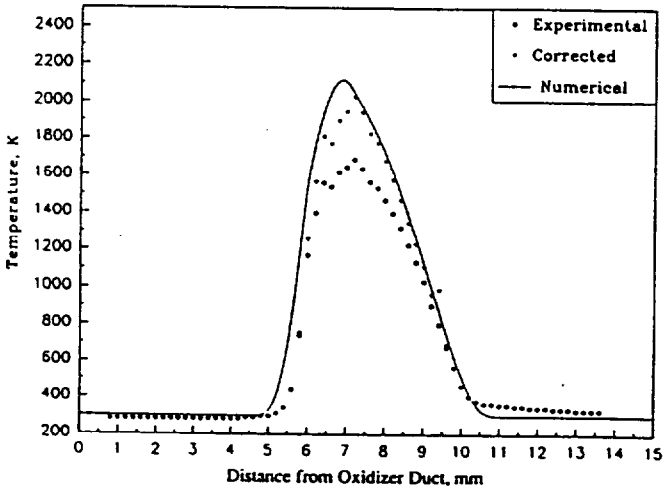

3. *The measured (points) and calculated (line) temperatures in the flame with 5% CH_3Cl added to the oxidizer stream. Uncorrected (circles) and radiation corrected data (triangles) are also shown.*

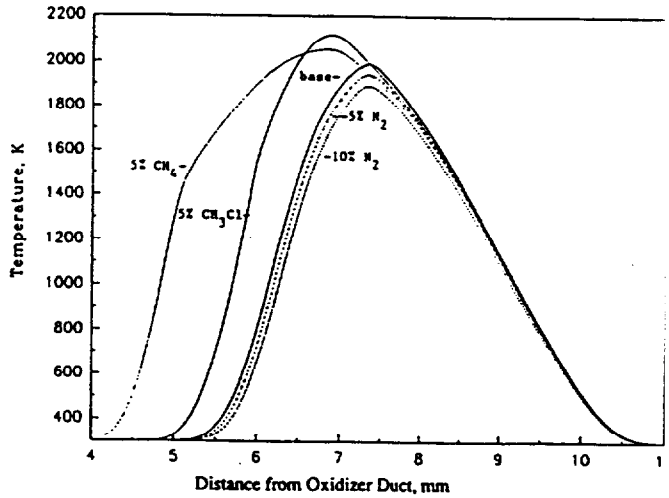

4. *The calculated temperature profiles for the base flame and for the flames with 5% N_2, 5% CH_3Cl and 5% CH_4 added to the oxidizer stream.*

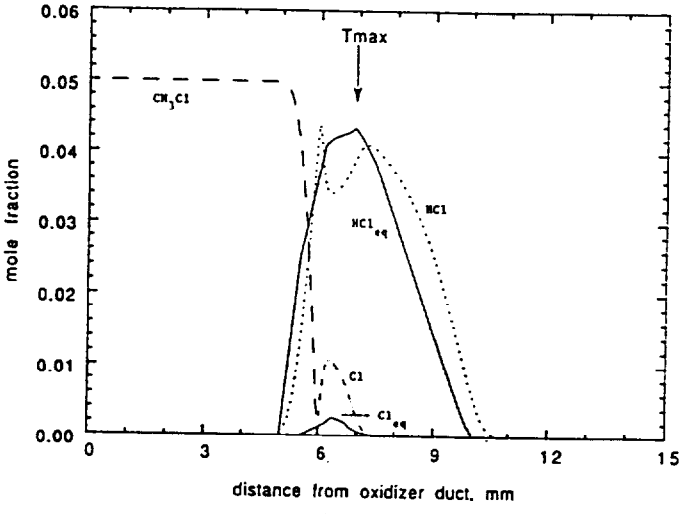

5. The calculated concentration of major chlorinated species in the 5% CH_3Cl flame. Complete local equilibrium for HCl and Cl are also shown.

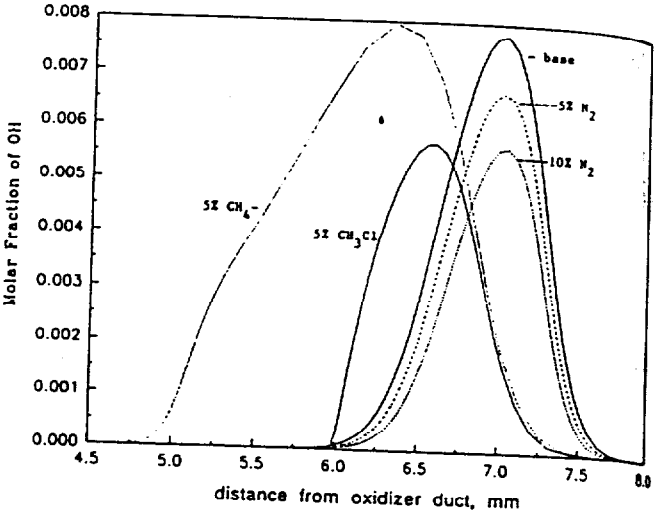

6. The calculated concentration of OH in the base flame and the flames with 5% N_2, 10% N_2, 5% CH_3Cl and 5% CH4 added to the oxidizer.

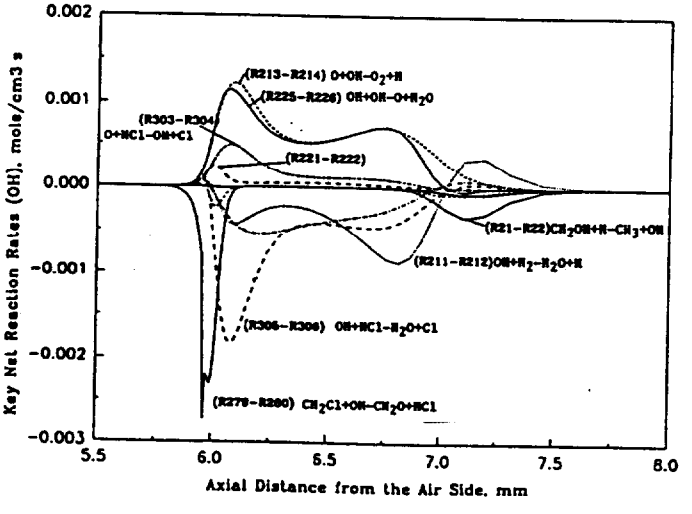

7. The calculated major net OH production and destruction reactions in the flame with 5% CH_3Cl added to the oxidizer stream.

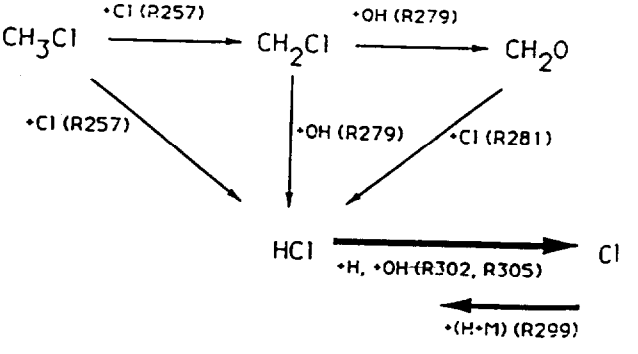

8. A schematic representation of the dominant chemical pathways involved in CH_3Cl pyrolysis.